JOURNAL OF Applied Polymer SCIENCE

The Electrorheological Properties of Polyaniline Nanofiber/Kaolinite Hybrid Nanocomposite

Baoxiang Wang,[1,2] Chenjie Liu,[1] Yichao Yin,[1] Xiaoli Tian,[1] Shoushan Yu,[1] Kezheng Chen,[1] Pengbo Liu,[2] Bing Liang[2]

[1]College of Materials Science and Engineering, Qingdao University of Science and Technology, Qingdao 266042, China
[2]State Key Laboratory of Polymer Materials Engineering, Sichuan University, Chengdu 610065, China
Correspondence to: B. Wang (E-mail: bxwang@qust.edu.cn) or K. Chen (E-mail: kchen@qust.edu.cn)

ABSTRACT: A novel polyaniline nanofiber/kaolinite nanoplatelet hybrid nanocomposite was synthesized by means of rapidly mixed *in situ* polymerization. The resultant polyaniline/kaolinite hybrid nanocomposite was characterized via different techniques, such as X-ray diffraction, thermogravimetric analysis, Fourier transform infrared spectroscopy, scanning electron microscopy, and transmission electron microscopy. The results show that 2D clay nanoplatelets are coated by the 1D polyaniline nanofibers. The nanoclay platelets can improve the thermal stability of polyaniline nanofibers. An electrorheological effect is found with the suspension of polyaniline nanofiber/kaolinite nanoplatelet hybrid nanocomposite dispersed in silicone oil. © 2013 Wiley Periodicals, Inc. J. Appl. Polym. Sci. 130: 1104–1113, 2013

KEYWORDS: conducting polymers; nanostructured polymers; properties and characterization; rheology

Received 21 January 2013; accepted 12 March 2013; Published online 17 April 2013
DOI: 10.1002/app.39262

INTRODUCTION

Organic–inorganic hybrid materials, composed of polymers and inorganic materials such as metal oxides and mica-type silicates, have recently received considerable attention due to their unique properties, e.g., high performance engineering materials with enhanced stiffness, strength, two-dimensional stability, and mechanical, thermal, electrical, and optical characteristics.[1–4] Organic–inorganic hybrids, especially the low-dimensional hybrid may provide further novel functions that integrate the peculiarity of different nanomaterials.

Due to the high conductivity, environmental stability, lower cost, and easy processability, conjugated conducting polymers, especially polyaniline (PANI), are promising materials for future applications in molecular electronics, wires, chemical sensors, and devices.[5,6] The electrical conductivity of conducting polymer materials can be reversibly controlled over many orders of magnitude via, e.g., doping and de-doping process.[7,8] Certain conducting polymeric materials, e.g., polyaniline, also have mechanical flexibility and environmental stability, which make the conducting polymer nanowires an ideal choice as building blocks of active circuit elements for the future ultraminiaturized nanoelectronic devices. Furthermore, the conductivity can be controlled chemically, making conducting polymer nanowires also promising sensing materials for ultrasensitive, trace-level biological and chemical nanosensors. Nanostructures of polyaniline are of great interest since they combine the properties of low-dimensional organic conductors with high surface area. Polyaniline nanostructures, such as nano-fibers/-wires/-rods/-tubes, can be made by introducing "structural directors" into the chemical polymerization bath. These structural directors include "soft templates" such as surfactants, organic dopants, or polyelectrolytes that assist in the self-assembly of polyaniline nanostructures, and "hard templates" such as porous membranes or zeolites where the templated polymerization of aniline occurs in the 1-D nanochannels.[9–13] Nanostructured polyaniline can also be made by electrospinning, electrochemical method, and template-free method.[14,15] Although micro- and nano-structures of PANI have been prepared by so many methods, so far, few publications have reported the preparation of polyaniline/clay low-dimensional hybrid.

Kaolinite, one of the most ubiquitous clay minerals on the earth, is a hydrated aluminium silicate possessing the ideal composition $Al_2Si_2O_5(OH)_4$. Moreover, kaolinite is a 1:1 dioctahedral clay mineral whose structure is composed of interstratified $AlO_2(OH)_4$ octahedral sheets and SiO_4 tetrahedral sheets. Each layer contains a sheet of SiO_4 tetrahedral forming six-membered silicate rings connected to the sheet of AlO_6 octahedral through the apical oxygens.[16,17] Kaolinite, as opposed to montmorillonite (MMT),

has very low cation exchange capacities. So kaolinite has been described as the non-expandable clay. Until now, only a limited number of polar guest species, such as *N*-methylformamide (NMF), potassium acetate, and dimethyl sulfoxide (DMSO), can be intercalated directly.[18,19] Although not many compounds have the ability to intercalate, the number may be extended by the so-called "displacement method." Displacement involves the replacement of a directly intercalated species (e.g., NMF or potassium acetate) by a second organic molecule. The use of a directly intercalating compound as an intermediate for the intercalation of other polar organic compounds opens up new areas for basic, strategic, and applied research.[20–22] The resultant hybrid materials combine the features of the clay and of the guest species. Recently, many examples of polymer intercalated aluminosilicate have been reported, which mainly focus on the montmorillonite. In spite of kaolinite's great abundance, high crystallinity, and high purity when compared with mineral clays (MMT), only few example of kaolinite intercalation with organic polymers has been reported. Efficient modifications have also been reported for the kaolinite, for instance poly(ethylene glycol) (PEG), *n*-methyl formamide (NMF), 1-methyl-2-pyrrolidone, or 6-aminohexanoic acid (AHA), Ethylene-vinyl alcohol (EVOH), etc.[23–27] Furthermore, polyaniline nanofiber/kaolinite is seldom researched.

In this study, we describe the synthesis of polyaniline nanofiber/kaolinite nanoplatelet nanocomposite and show the usefulness of hybrid in generating such a novel material. The influence of the composition on the morphology and structure of polyaniline nanofiber/kaolinite 2D nanoplatelet nanocomposite was investigated.

EXPERIMENTAL

Materials

The kaolinite sample ($Al_2Si_2O_5(OH)_4$) employed in this study was from Shanghai, China (Shanghai Fengxian Fengcheng Reagent Factory). It was received as a finely divided white powder of high purity, and its chemical composition in wt % as oxide is SiO_2, 48.97; Al_2O_3, 34.22; Fe_2O_3, 0.6; and TiO_2 0.27. The specific surface area is 26 m^2/g. The kaolinite was used without further purification. Aniline monomer (AN, Tianjin Bodi Chemicals.) was distilled under reduced pressure before use. Ammonium persulfate (APS; 99.99%, Beijing Chemicals), Poly(vinyl pyrrolidone) (PVP), and hydrochloric acid were used as received.

Synthesis of Polyaniline Nanofibers/Kaolinite Nanoplatelet Nanocomposite by Modified Rapid Mixing Method

Reactions were generally carried out in 250 mL three-necked flask. HCl was used as the dopant. APS was used as the initiator to initiate the in-situ polymerization. PVP was used as a dispersant to make kaolinite form a stable aqueous and increase the binding between PANI and kaolinite. Rapidly mixed *in situ* polymerization is used as synthesized approach. Typically, different amounts of kaolinite (kaolinite/aniline = 0%, 5%, 10%, 15%, 20%, 50%) and 0.5 g PVP were added into an aqueous solution of aniline (19.2 mmol) in 1 mol/L HCl doping acid (60 mL). The suspension was stirred for 8 h under 80°C. Another solution of ammonium peroxydisulfate (4.8 mmol) in the same doping acid (60 mL) was prepared. The molar ratio of aniline to APS was kept at 4:1. Rapid-mixing reactions were performed by pouring the two solutions together and immediately stirring to ensure sufficient mixing before polymerization begins. Polymerization can be observed when the characteristic green color of polyaniline emeraldine salt became visible. After 0.5 h the product was filtered with a Buchner funnel possessing filter paper and washed with deionized water, and then dried in vacuum at 80°C for 4 h to obtain a green-black PANI/kaolinite powder.

The Preparation of ER Suspensions

ER properties were measured as follow: first, PANI/kaolinite powder was further immersed in 1*M* aqueous NH_3 solution for overnight to do a dedoping treatment. The purpose for this is to control the conductivity from conductive to semiconductive, which make it useful for ER application. Second, the PANI/kaolinite nanohybrid particles were obtained via the process of filtering, washing, drying (80°C 12 h) and crushing with a mortar. The obtained particles were crushed in a mortar and mixed with silicone oil. The silicone oil (dielectric constant $\varepsilon_f = 2.72 \sim 2.78$, density $\rho = 0.966 \sim 0.974$ $g{\cdot}cm^{-3}$, viscosity $\eta = 500$ $mm^2{\cdot}s^{-1}$) was first dried at 100°C for 2 h, and then ERFs were prepared by dispersing the particles into the silicone oil (at particles:silicone oil = 10 wt %). Time elapsed after the preparation of the polyaniline/kaolinite ER fluid before the start of rheological testing is about 0.5 h. It includes two parts: one is that crushing polyaniline/kaolinite particles into a mortar for about 10 min, another is then crushing polyaniline/kaolinite particles in silicone oil for 20 min. The aim of short time before rheological testing is to avoid the adsorption of moisture from atmosphere, which may have influence on the measurement of ER testing.

Characterization

Transmission electron microscopy (TEM) experiments were performed using a Philips Tecnai G^2 20 microscope operating at 200 kV. The samples were prepared by depositing a drop of the suspension onto a porous carbon grid. The phase composition and crystallinity of the synthesized powders described above were characterized via X-ray powder diffraction (XRD, D/Max 2400, Rigaku, Tokyo, Japan; equipped with graphite monochromatized CuKα radiation) in the 2θ angle ranging from 4° to 50°. The morphology of the particles was observed by scanning electron microscopy (FESEM, Hitachi S-4700). To analyze the thermal stability and mass percent of samples, thermogravimetric analyzer STA449c (TGA, NETZSCH-Ger tebau GmbH, Germany) was utilized with a heating rate of 10°C min^{-1} from room temperature up to 800°C in N_2 atmosphere. FT-IR spectra were recorded on a Fourier transform infrared spectrometer (FT-IR, KBr disk method; NEXUS) at wavenumbers 400−4000 cm^{-1}. A modified rotary viscometer (NXS-11A; Chengdu, China) and a high-voltage DC power source (DPS-100; Da Lian, China) were used to research the rheological properties of ER fluids.

RESULTS AND DISCUSSION

The Morphological Study of Polyaniline Nanofiber/Kaolinite Particles

The morphology of pure kaolinite and polyaniline nanofiber/kaolinite particles is shown in Figure 1. It can be seen that unmodified kaolinite is composed of small aggregated platelets (1–10 μm). The stack of platelets and sharp edges are clearly

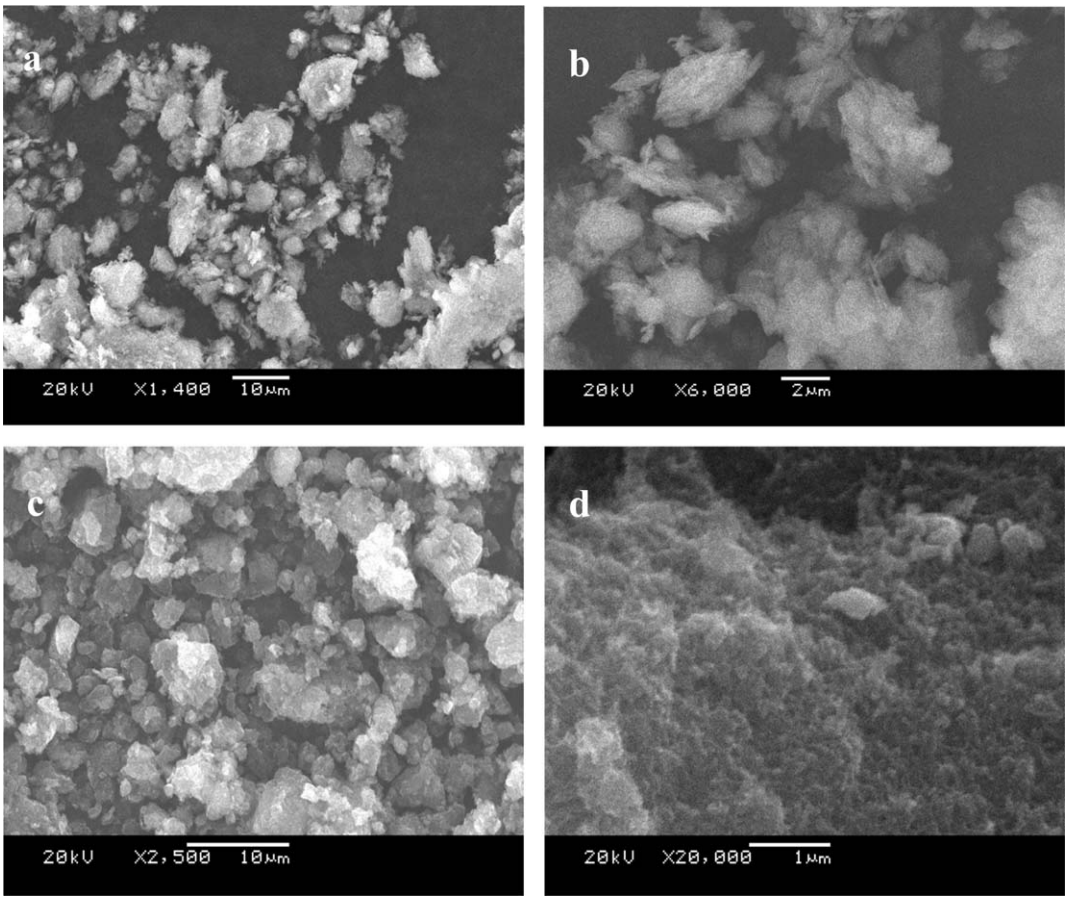

Figure 1. SEM image of (a,b) pure kaolinite and (c,d) PANI nanofibers/kaolinite nanocomposite.

shown. However, polyaniline nanofiber/kaolinite nanocomposite particles be seen in Figure 1(c,d) looking very different. The shape of particles is irregular-polyhedron and it shows filled edges and corners. The size is enlarged due to the polyaniline coated on the surface of kaolinite. Furthermore, roughness surface of polyaniline nanofiber/kaolinite nanocomposite particles verify the existence of polyaniline nanofibers.

TEM images of pure PANI nanofibers (a,b) and PANI nanofibers/kaolinite nanocomposite (c–f) were showed in Figure 2. PANI nanofibers are produced via rapidly mixed polymerization. The transmission electron microscopy (TEM) images clearly show that the polyaniline fibers had a diameter of about 20–30 nm and lengths varying from 500 nm to several micrometers (As shown in Figure 2 a and b). Polyaniline fibers, unlike inorganic nanorod, are soft and easy aggregated together. TEM images of polyaniline nanofiber/kaolinite hybrid after *in situ* polymerization treatment is shown different morphology. Polyaniline nanofibers coated on hexagons nanoplate of kaolinite were clearly observed. Kaolinite with typical sheet-like structure is shown morphology with well-defined hexagonal edges and corner angles (120°). PANI nanofibers can be anchored on the external surfaces of the clay sheets. Comparing with pure PANI nanofibers, the size and length of the PANI chains anchored to the platelet surface is a little smaller and shorter (estimated about 20 nm diameter and 200–400 nm length). If too much AN were used to polymerized and PANI be coated on the surface as shown as TEM Figure 2(g–i), there appear thicker PANI coating and PANI nanofibers also can be found around the clay sheets. Previously, a modified interfacial polymerization was used to prepare PANI/bentonite nanohybrids in our group.[28] By an interfacial polymerization, the monomer and initiator existed in different phases, which ensured the successful synthesis of the PANI nanofibers. However, some bentonite particles sedimented at the interface due to its high density and this may prohibit the aniline monomer dispersing into the oil phase. Furthermore, aniline monomer and bentonite were separated at different phase; the formation of PANI/bentonite coating structure is difficult. Therefore, in this research, rapidly mixed *in situ* polymerization was used to prepare polyaniline/kaolinite hybrid nanocomposite. Both aniline monomer and kaolinite were existed into the same reaction system, which is helpful to form a core/shell or coating structure.

XRD Analysis

Figure 3 shows the XRD patterns of pure PANI nanofibers, pure kaolinite, and a series of PANI nanofibers/kaolinite composites. Pure PANI nanofibers exhibit crystallization partly. The characteristic peaks centered at $2\theta = 18°$ and 25° are observed in PANI nanostructures, and are attributed, respectively, to the periodicity perpendicular and parallel to the polymer chain, which means partly crystallined PANI. Characteristic maximal of raw kaolinite are observed at $2\theta = 12.6°$ (very intense, sharp, and narrow), which is corresponded to the basal spacing of kaolinite (0.715

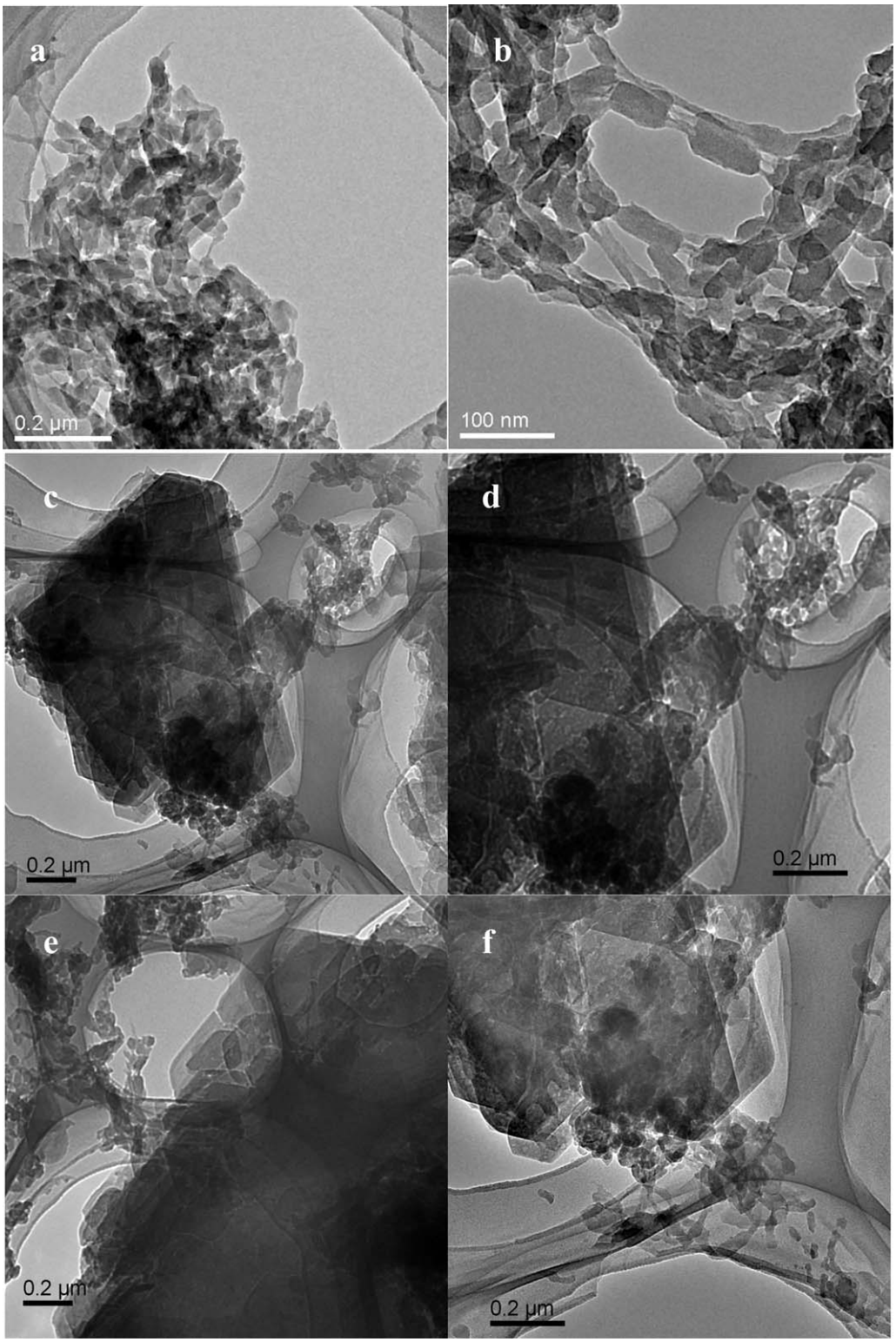

Figure 2. TEM images of (a,b) pure PANI nanofibers and (c–i) PANI nanofibers/kaolinite nanocomposite.

nm). Interestingly, polyaniline nanofiber/kaolinite nanoplatelet hybrid nanocomposite is found with special structure. The main peaks of PANI and kaolinite are retained after the hybrid treatment. The peak at $2\theta = 12.6°$ in the original kaolinite, assigned as the first basal peak d_{001}, is not shift to small reflection angles. This result shows that PANI is not intercalated into the interlayer space of kaolinite due to the small basal spacing and its strong hydrogen bonding between the sheets. Furthermore, the intensities of the d_{001} peaks decreased rapidly with the increasing content of PANI, and the intensity of the PANI peaks were

Applied Polymer SCIENCE

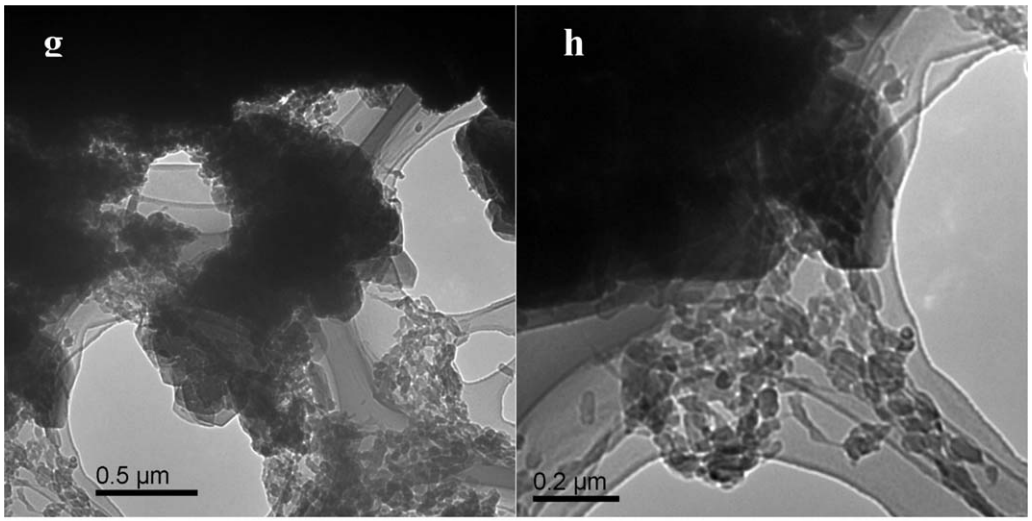

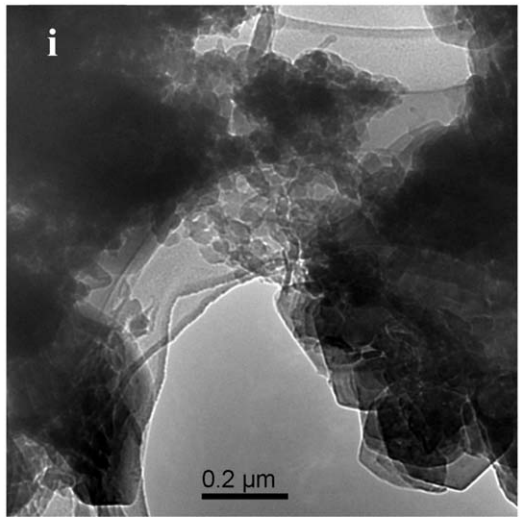

Figure 2. (continued from the previous page)

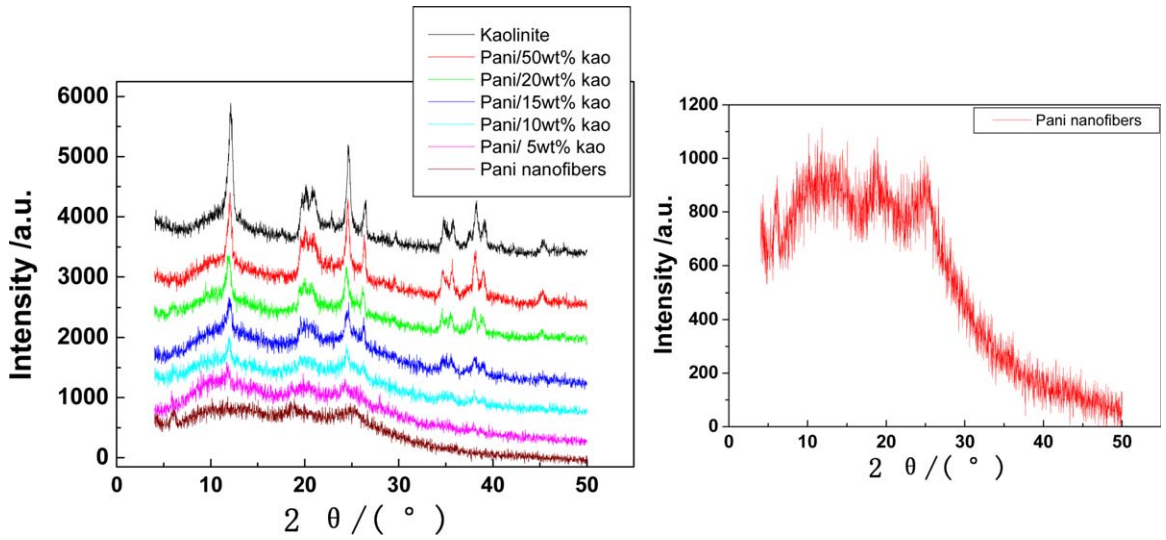

Figure 3. XRD patterns of pure PANI nanofibers, pure kaolinite, and a serial of PANI nanofibers/kaolinite composite. Right curve is the XRD of pure PANI nanofibers. [Color figure can be viewed in the online issue, which is available at wileyonlinelibrary.com.]

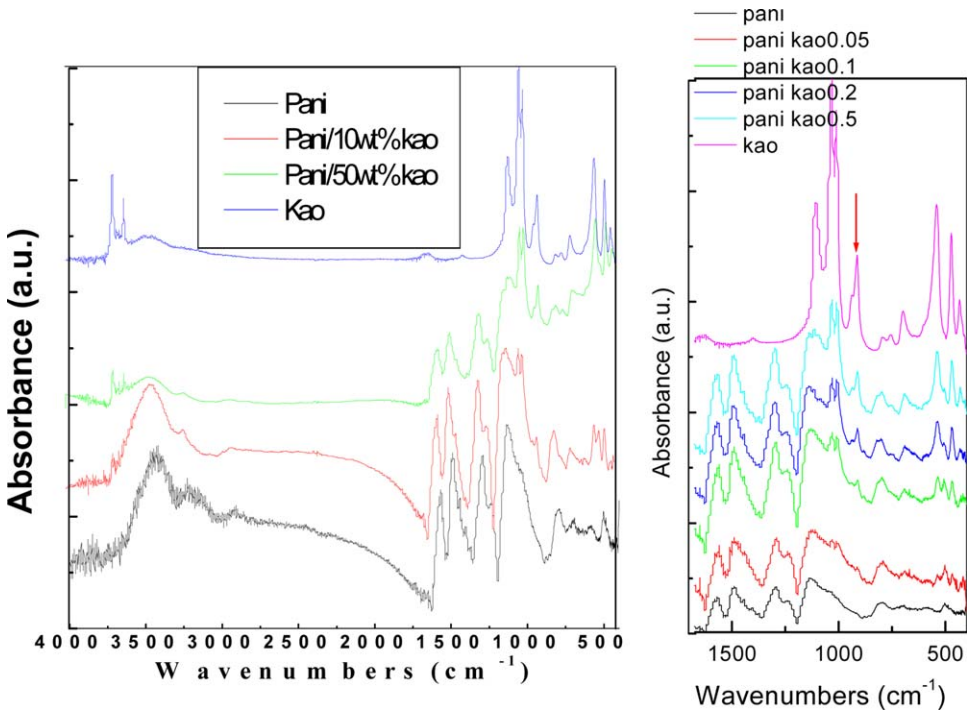

Figure 4. FTIR spectra of pure PANI nanofibers, serials of PANI nanofibers/kaolinite composite, pure kaolinite (from bottom to top). [Color figure can be viewed in the online issue, which is available at wileyonlinelibrary.com.]

enhanced, simultaneously. The strong characteristic d_{001} peak of raw kaolinite (at $2\theta = 12.6$) is used to do the peak area analysis. The peak areas of seven samples are 2475, 2180, 1992, 1937, 1901, 1855, and 1805, respectively. Therefore, the real kaolinite/PANI proportion obtained from peak area analysis can be 100, 55.9, 27.9, 19.7, 14.3, 7.4, and 0 wt %. There exist the difference between the real proportion and feeding ratio.

FT-IR Analysis

The FTIR spectrum (Figure 4) shows the characteristic peaks of pure PANI nanofibers around 1572 (C=C stretching deformation), 1485 (vibration band of the benzenoid ring), 1296, 1120, and 799 cm^{-1}. Moreover, the vibration bands of C–H near 3400 cm^{-1} are also very strong. The IR absorption bands of kaolinite at 3694, 3670, 3654, and 3621 cm^{-1} are attributed to O–H stretching vibrations, those at 1114 and 1032cm^{-1} attributing to Si–O stretching vibrations and the peak at 913 cm^{-1} attributing to O–H deforming vibrations. The 3694, 3670, and 3654 cm^{-1} bands are O–H stretching vibration bands of the interlayer surface of layered silicates and 3621 cm^{-1} band is the O–H stretching vibration of the internal structure of layered silicates. For the IR patterns of PANI nanofibers/kaolinite composite, the O–H deforming vibration of 913 cm^{-1} are moved to 910 cm^{-1} and weakened sharply accompanying the decreasing content of kaolinite. The Si–O stretching vibrations of kaolinite at 1114 cm^{-1} are decreased to a small peak and moved to 1150 cm^{-1}. These results showed that the O–H bands of the interlayer surface were disturbed and the layer of kaolinite may have interaction with the polar group of PANI.

TGA Analysis

Thermogravimetric analyses (TGA) were carried out under argon with a heating rate of 10°C/min in the temperature range from 30 to 800°C. Thermogravimetric analysis (TGA) was performed on among PANI nanofibers, pure kaolinite, and the PANI/10 wt %kaolinite nanocomposite to determine their thermal stabilities under nitrogen atmosphere. In Figure 5, the thermal treatment of kaolinite may be considered as taking place in two steps. The first step up to 100°C is water desorption step. Such dehydration depends on the nature of the kaolinite and the degree of disorder of stacking. After dehydration, the kaolinite goes through a pre-dehydroxylation state. In the temperature range between 450 and 550°C, the kaolinite dehydroxylates and the product phase is known as metakaolinite. The following reaction may be envisaged: $Al_2(OH)_4Si_2O_5 \rightarrow Al_2Si_2O_7 + 2H_2O$.

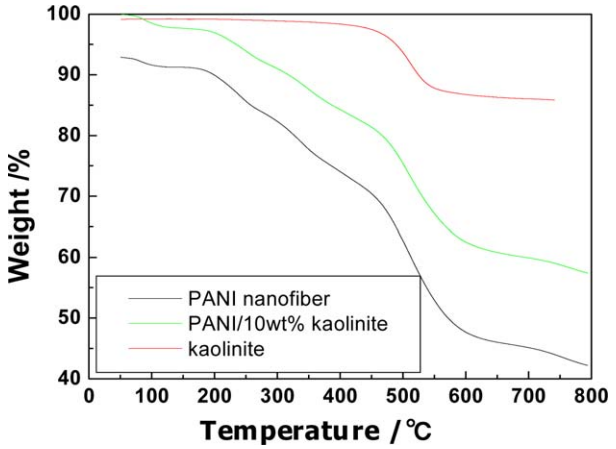

Figure 5. TGA curves of (a) PANI, (b) PANI/10 wt %kaolinite, and (c) kaolinite. [Color figure can be viewed in the online issue, which is available at wileyonlinelibrary.com.]

In Figure 5, 58% of mass was lost for the pure PANI and 44% of mass was lost for the PANI/10 wt %kaolinite nanocomposite when the experiment was terminated at 800°C. In the measured temperature range, the weight loss of PANI/10 wt %kaolinite nanocomposite is lower than that of pure PANI nanofibers. Increased thermal stability of the PANI/10 wt %kaolinite nanocomposite could be due to the existence of inorganic clay nanolayers.

ER Behavior of PANI/Kaolinite Nanocomposite Suspension

Electrorheological fluids (ERFs), a kind of smart materials, are suspensions of micro- and/or nano-sized dielectric particles dispersed in a non-conductive liquid and exhibit drastic changes in their rheological properties, which include a large increase in apparent viscosity, yield stress, shear stress, storage modulus, loss modulus, etc., and the formation of reversible fiber and chain microstructures under an external applied electric field.[29–37] Particle polarization is now widely thought to be responsible for the interaction force that lead to the rheological change of ER fluids. Application of an electric field can induce polarization of the suspended particles and a chainlike structure can be formed along the electric field direction in a few milliseconds. ER characteristics find practical applications in many fields. However, low shear stress, poor temperature effect, rapid sedimentation, leaking current, etc., have been limited the industry application. Recently, some new applications have been expanded, such as actuators, shock absorbers, active devices, human muscle simulators, ER tactile displays, photonic crystal, seismic controlling frame structures, etc.[38–40]

Since the first report on PANI–clay nano-composite-based ER fluids from an emulsion polymerization method, polymers (e.g., PANI, PPy, and styrene–acrylonitrile copolymer) and clay (e.g., montmorillonite, halloysite, and kaolinite) nanocomposites have been extensively used as suspended particles, taking advantage of either hydrophobic or hydrophilic surface characteristics of clay. In previous study, polymer chains are inserted between the layers with an extended single chain conformation to form a so-called intercalation structure.[41,42] Until now, except intercalated structure PANI, other nanostructure PANI have been used as a ER materials due to its much smaller size, good physical and chemical properties. Recently, Yin et al. reported a PANI nanofiber (PANIF) based ER fluid with higher yield stress and reduced sedimentation, which indicated a superior candidate for ER fluid. Pure PANI nanofibers and their composite, e.g., coaxial cable-like PANI@titania nanofibers, silica nanoparticle decorated polyaniline nanofiber, have been also investigated.[43,44] Various clay minerals have been adopted in the field of polymer–clay composites, and Choi et al. have reported the fabrication of polyaniline/clay and polyaniline particles wrapped by exfoliated clay sheets and studied their electrorheological (ER) properties. Halloysite nanotube (HNT), two-layered aluminosilicate clay mined from natural deposits is chemically similar to kaolinite. The material exhibits unique chemical properties owing to its hollow nanotubular structure, i.e., the outer and inner surface has properties similar to SiO_2 and Al_2O_3, respectively. As a new clay material, the unique hollow nanotubular structure of HNT is expected to play an important role in the HNT–polymer composite-based ER materials.[45]

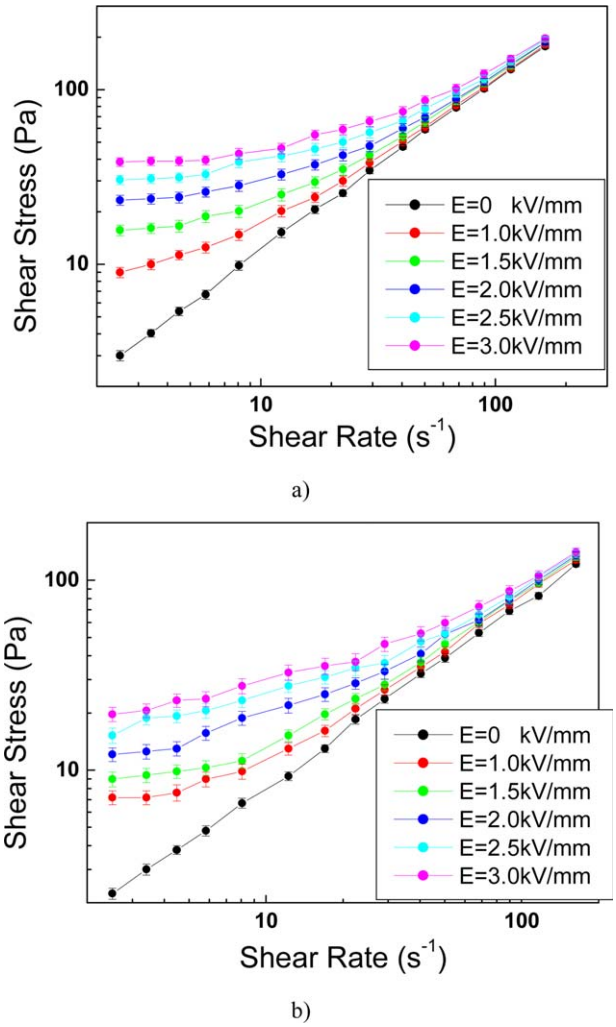

Figure 6. Shear stress as a function of shear rate for the suspension of (a) PANI/10 wt %kaolinite and (b) PANI/15 wt %kaolinite particles, respectively. [Color figure can be viewed in the online issue, which is available at wileyonlinelibrary.com.]

Kaolinite is an aluminosilicate with the ideal composition $Al_2Si_2O_5(OH)_4$. Moreover, kaolinite is a 1:1 dioctahedral clay mineral whose structure is composed of interstratified $AlO_2(OH)_4$ octahedral sheets and SiO_4 tetrahedral sheets. Consequently, the interlayer space is unsymmetrical, allowing particular reactions. Kaolinite does not have any ions, while layered silicate including MMT possesses exchangeable cations which makes an intercalated structure with PANI. However, kaolinite has regular hexagonal shape nanoplate and polar group on the surface (hydroxyl). There exist three inner surface hydroxyl and one inner hydroxyl group per crystal unit cell of kaolinite. The hydrogen bonding between surface hydroxyl groups of kaolinite and amino of PANI may play a significant role for enhancing the interaction.

The shear stresses of PANI/kaolinite particles ERF as a function of shear rate under various electric fields are shown in Figure 6. The suspension has good rheological properties in the range of shear rate, the shear stress of the suspension increases with the shear rate. With the absence of electric field, the flow behavior

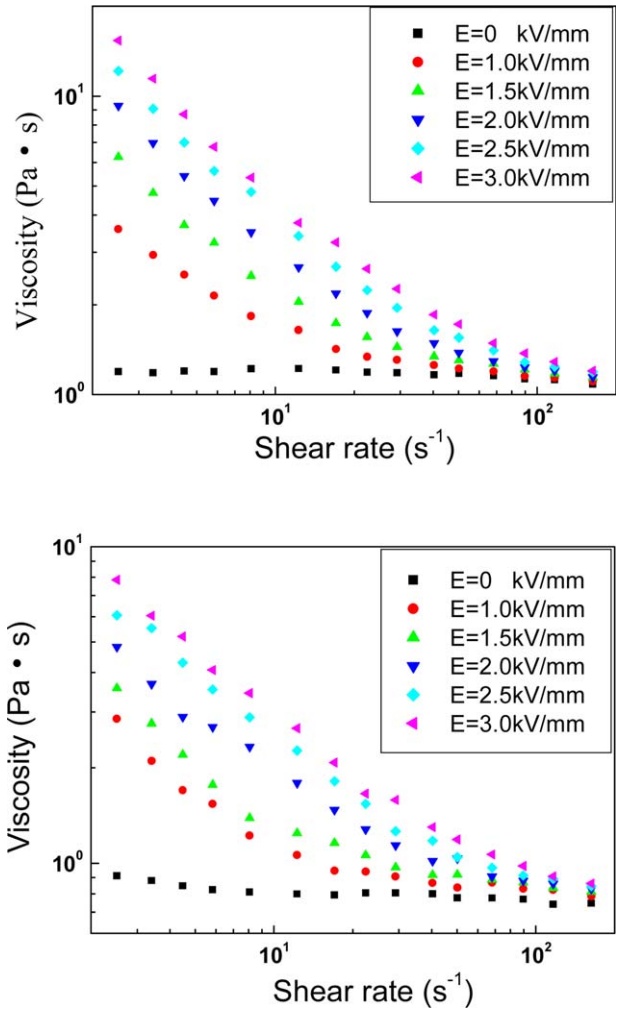

Figure 7. Viscosity curves versus shear rate for PANI/10 wt %kaolinite (top) and PANI/15 wt %kaolinite (down) particles based on ER fluids (10 wt %) under various electric field strengths, respectively. [Color figure can be viewed in the online issue, which is available at wileyonlinelibrary.com.]

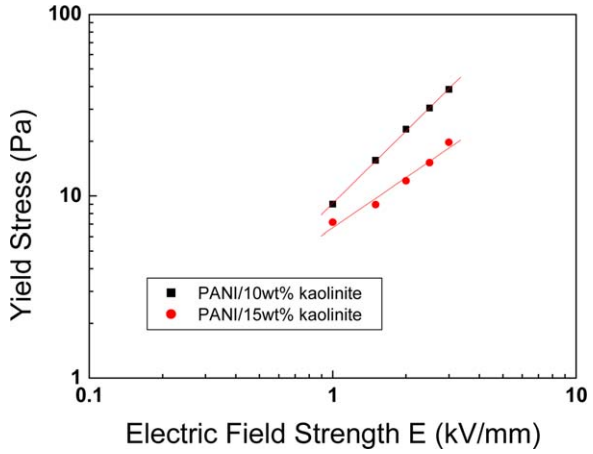

Figure 8. Yield stress as a function of electric field strength for the Suspension of PANI/10 wt %kaolinite and PANI/15 wt %kaolinite particles, respectively. [Color figure can be viewed in the online issue, which is available at wileyonlinelibrary.com.]

of suspensions made of PANI/kaolinite hybrid particles shows a Newtonian fluid behavior. In the presence of an electric field, Bingham plastic behavior can be observed in the composite suspension, which is the typical rheological characteristic of ERFs under an electric field.[46–57] Figure 6 also shows the behavior of the shear stress of ERF with an increase of the DC electric field. The particle fraction is 10 wt % in silicone oil. When the electric field is applied, yield stresses appear and increase step by step with the stepwise increase of an applied electric field strength. Comparing PANI/15 wt %kaolinite hybrid, PANI/10 wt %kaolinite hybrid based ER fluid exhibits higher shear stresses and more stable ER behavior.

The ER efficiency is defined by $(\tau_E - \tau_0)/\tau_0$, where τ_E is the static yield stress with an electric field, and τ_0 is the static yield stress at zero field. The ER efficiency for the PANI/10 wt %kaolinite hybrid suspensions, and the PANI/15 wt %kaolinite hybrid suspension is 6.728 and 5.272 under electric field strength $E = 2.5$ kV/mm, respectively. The PANI/10 wt %kaolinite hybrid suspensions have the highest ER efficiency (10 wt % in silicone oil). Furthermore, comparing our previous study, the ER efficiency for the PANI/ bentonite hybrid suspensions is only 4.19, whereas its particles weight fraction to silicone oil is as high as 20 wt %. Therefore, PANI/10 wt %kaolinite hybrid suspensions have better ER effect than that of PANI/bentonite hybrid suspensions. In this study, PANI/10 wt %kaolinite hybrid was synthesized via a rapid mixing *in situ* polymerization and polyaniline nanofibers coated on hexagons nanoplate of kaolinite was clearly shown. Nanosized two-dimensional clay plate and one-dimensional nanofibers form a special hybrid structure, which is suitable to increase ER effect.

Viscosity curves versus shear rate for PANI/10 wt %kaolinite and PANI/15 wt %kaolinite particles based on ER fluids (10 wt %) under various electric field strengths, respectively, is shown in Figure 7. The shear viscosity of both fluids increase with increasing electric field strength at the same shear rate. This is a typical ER solidification from liquid state to solid state. Non-Newtonian performances are observed in Figure 7, where the ER fluid shows typical shear thinning phenomenon at each electric field as compared to the uniform viscosity at zero field strength, which is the characteristics of shear viscosity decrease with the increasing shear rate. These phenomena are mainly associated with the change of microstructure of chains formed by polarized PANI/kaolinite particles in silicone oil. Under an electric field, the electrostatic forces cause the dispersed PANI/kaolinite particles to form chains or columns along the electric field direction; the reformation and destruction rate of particle chains depend on the competition between electrostatic and hydrodynamic forces. The breaking and re-formation process caused by the cooperation of electrostatic and hydrodynamic interactions are reduced by an external electric and flow field.

The yield stress (τ_y) as a function of electric field strengths (E) is shown in Figure 8. In which τ_y yield stress is the extrapolated value obtained from flow curve in Figure 6. The dynamic yield stress versus electric field strength for different PANI/kaolinite hybrid particles (10 wt % particle concentration) based ER fluid is obtained. In general, the dependency of the dynamic yield

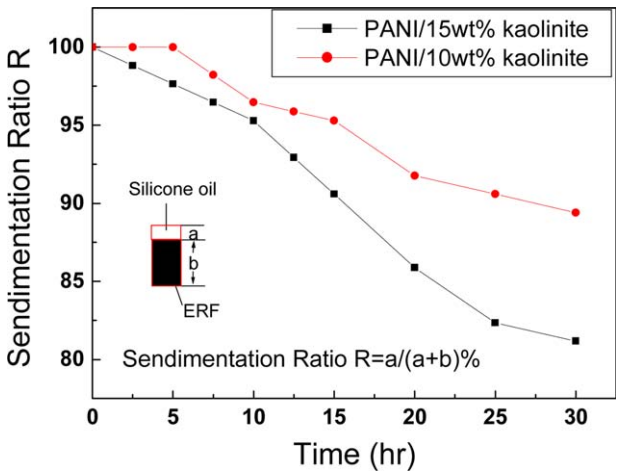

Figure 9. Sedimentation properties of two different types of PANI/kaolinite based ER fluids [inset: definition of sedimentation ratio]. [Color figure can be viewed in the online issue, which is available at wileyonlinelibrary.com.]

stress on the electric field strength was presented by the power law relationship as follows: $\tau_y E^m$.[58,59] Compared to the suspension containing PANI/15 wt %kaolinite composite particles, the suspension containing PANI/10 wt %kaolinite composite particles exhibits a higher yield stress (Figure 8), indicating a higher solidification. The *m* value of PANI/10 wt %kaolinite composite suspension is higher than that of PANI/15 wt %kaolinite composite particles suspension. The values of *m* are normally between 1 and 2. If its value is as high as 2 or 1.5, which are predicted by the classic polarization model and conduction model. Therefore, the change of *m* value may provide the variance of ER mechanism. The leaking current density of ER fluid is regarded as the other main factor in practical application, because the ER fluids with higher current density will consume more power and even breakdown under high electric field strength. Both two kinds of PANI/kaolinite hybrid ERF have small current density, which is below 10 $\mu A/cm^2$ at $E = 3$ kV/mm. This may provide another useful property for the application of this type ERF.

The stability of ER materials plays an important role in the ER application. The properties of the ERF decrease abruptly with the increase of the sedimentation. Although the sediment particles can be re-dispersed into silicone oil after the slightly shaking and it can get similar result after several time's reusable measurement, it is better to enhance the anti-sedimentation of ER suspension. The normal method taken to enhance the anti-sedimentation of ERF may include: smaller particle size (e.g., nanotube, nanofiber, nanorod, nanoparticle, etc), hollow or porous structure, matching the densities of the particles and oil and adding surfactant to enhance the stability of ERF. In this study, the sedimentation ratio of particles in the silicone oil was measured as shown in Figure 9. In the dispersion stability test, PANI/10 wt %kaolinite based ER showed a better dispersion stability for a long time. PANI nanofiber and 2D clay nanoplate are better to enhance the stability of ER fluid. In future, low-dimensional hybrid (such as 2D/1D, 1D/1D, 1D/0D, etc.) is worthwhile to investigate deeply for ER materials. Their special structure is beneficial not only to enhance the ER activity, but also anti-sedimentation behavior.

CONCLUSIONS

In summary, concerning composition, low loadings of clay, i.e., 10 wt %, provided improved nanodispersed morphologies and property improvements: increased thermal stability, crystallinity with respect to the neat PANI. The flow behavior of suspensions made of PANI/kaolinite hybrid particles shows a Newtonian fluid and Bingham behavior with and without external DC electric field. From the above results, it can be generally concluded that there is great potential for these nanocomposites to become implemented in applications. This facile method provides a novel path for the design of the low-dimensional hybrid.

ACKNOWLEDGMENTS

We gratefully acknowledge financial support from the National Natural Science Foundation of China (NSFC 51072087), the Project Sponsored by the Scientific Research Foundation for the Returned Overseas Chinese Scholars, the Opening Project of State Key Laboratory of Polymer Materials Engineering (Sichuan University) (KF201303) and Shandong Distinguished Middle-aged and Young Scientist Encourage and Reward Foundation (BS2011CL016).

REFERENCES

1. Giannelis, E. P. *Adv. Mater.* **1996**, *8*, 29.
2. Wang, J. F.; Severtson, S. J.; Stein, A. *Adv. Mater.* **2006**, *18*, 1585.
3. Bitinis, N.; Hernandez, M.; Verdejo, R.; Kenny, J. M.; Lopez-Manchado, M. A. *Adv. Mater.* **2011**, *23*, 5229.
4. Bafna, A.; Beaucage, G.; Mirabella, F.; Mehta, S. *Polymer* **2003**, *44*, 1103.
5. Huang, J. X.; Kaner, R. B. *Chem. Commum.* **2006**, *4*, 367.
6. Huang, J. X. *Pure Appl. Chem.* **2006**, *78*, 15.
7. Zhang, W. L.; Park, B. J.; Choi, H. *J. Chem. Commun.* **2010**, *46*, 5596.
8. Cheng, Q. L.; Pavlinek, V.; He, Y.; Li, C. Z.; Saha, P. *Colloid Polym. Sci.* **2009**, *287*, 435.
9. Chiou, N. R.; Epstein, A. *J. Adv. Mater.* **2005**, *17*, 1679.
10. Ma, Y. F.; Zhang, J. M.; Zhang, G. J.; He, H. X. *J. Am. Chem. Soc.* **2004**, *126*, 7097.
11. Zhang, Z. M.; Wan, M. X.; Wei, Y. *Adv. Funct. Mater.* **2006**, *16*, 1100.
12. MacDiarmid, A. G.; Jones, J. W. E.; Norris, I. D.; Gao, J.; Johnson, J. A. T.; Pinto, N. J.; Hone, J.; Han, B.; Ko, F. K.; Okuzaki, H.; Llaguno, M. *Synth. Methods* **2001**, *119*, 27.
13. Zujovic, Z. D.; Wang, Y.; Bowmaker, G. A.; Kaner, R. B. *Macromolecules* **2011**, *44*, 2735.
14. Xia, H. B.; Narayanan, J.; Cheng, D. M.; Xiao, C. G.; Liu, X. Y.; Chan, H. S. O. *J. Phys. Chem. B* **2005**, *109*, 12677.
15. Zhang, K.; Zhang, L. L.; Zhao, X. S.; Wu, J. S. *Chem. Mater.* **2010**, *22*, 1392.
16. Paul, D. R.; Robeson, L. M. *Polymer*, **2008**, *49*, 3187.
17. Frost, R. L.; Kristof, J.; Mako, E.; Martens, W. N. *Langmuir* **2002**, *18*, 6491.

18. Frost, R. L.; Horvath, E.; Mako, E.; Kristof, J.; Cseh, T. *J. Colloid Interface Sci.* **2003**, *265*, 386.
19. Takenawa, R.; Komori, Y.; Hayashi, S.; Kawamata, J.; Kuroda, K. *Chem. Mater.* **2001**, *13*, 3741.
20. Komori, Y.; Sugahara, Y.; Kuroda, K. *J. Mater. Res.* **1998**, *13*, 930.
21. Sun, D. W.; Li, Y. F.; Zhang, B.; Pan, X. B. *Compos. Sci. Technol.* **2010**, *70*, 981.
22. Komori, Y.; Sugahara, Y.; Kuroda, K. *Appl. Clay Sci.* **1999**, *15*, 241.
23. Komori, Y.; Sugahara, Y.; Kuroda, K. *Chem. Mater.* **1999**, *11*, 3.
24. Gardolinski, J. E.; Carrera, L. C. M.; Cantão, M. P.; Wypych, F. *J. Mater. Sci.* **2000**, *35*, 3113.
25. Letaief, S.; Detellier, C. *J. Mater. Chem.* **2005**, *15*, 4734.
26. Tunney, J. J.; Detellier, C. *Chem. Mater.* **1996**, *8*, 927.
27. Cabedoa, L.; Giméneza, E.; Lagaronb, J. M.; Gavarab, R.; Sauraa, J. *J. Polymer* **2004**, *45*, 5233.
28. Wang, B. X.; Yin, Y. C.; Liu, C. J.; Yu, S. S.; Chen, K. Z. *J. Appl. Polym. Sci.* **2012**, *128*, 1304.
29. Halsay, T. C. *Science* **1992**, *258*, 761.
30. Block, H.; Kelly, J. P. *J. Phys. D: Appl. Phys.* **1988**, *21*, 1661.
31. Tao, R.; Sun, J. M. *Phys. Rev. Lett.* **1991**, *67*, 398.
32. Gamota, D. R.; Filisko, F. E. *J. Rheol.* **1991**, *35*, 399.
33. Parthasarathy, M.; Klingenberg, D. *J. Mater. Sci. Eng. R* **1996**, *17*, 57.
34. Wen, W. J.; Huang, X. X.; Yang, S. H.; Lu, K. Q.; Sheng, P. *Nat. Mater.* **2003**, *2*, 727.
35. Hong, C. H.; Choi, H. J.; Jhon, M. S. *Chem. Mater.* **2006**, *18*, 2771.
36. Jin, H. J.; Choi, H. J.; Yoon, S. H.; Myung, S. J.; Shim, S. E. *Chem. Mater.* **2005**, *17*, 4034.
37. Shen, R.; Wang, X. Z.; Lu, Y.; Wang, D.; Sun, G.; Cao, Z. X.; Lu, K. Q. *Adv. Mater.* **2009**, *21*, 4631.
38. Hao, T. *Adv. Mater.* **2001**, *13*, 1847.
39. Wen, W. J.; Huang, X. X.; Sheng, P. *Soft Matter* **2008**, *4*, 200.
40. Liu, Y. D.; Choi, H. *J. Soft Matter* **2012**, *8*, 11961.
41. Kim, J. W.; Kim, S. G.; Choi, H. J.; Jhon, M. S. *Macromol. Rapid Commun.* **1999**, *20*, 450.
42. Choi, H. J.; Jhon, M. S. *Soft Matter* **2009**, *5*, 1562.
43. Yin, J.; Zhao, X.; Xia, X.; Xiang, L.; Qiao, Y. *Polymer* **2008**, *49*, 4413.
44. Liu, Y. D.; Fang, F. F.; Choi, H. *J. Soft Matter* **2011**, *7*, 2782.
45. Zhang, W. L.; Choi, H. *J. Colloid Polym. Sci.* **2012**, *290*, 1743.
46. Cao, J. G.; Huang, J. P.; Zhou, L. W. *J. Phys. Chem. B* **2006**, *110*, 11635.
47. Lengalova, A.; Pavlinek, V.; Saha, P.; Stejskal, J.; Kitano, T.; Quadrat, O. *Phys. A Stat. Mech. Appl.* **2003**, *321*, 411.
48. Espin, M. J.; Delgado, A. V.; Plocharski, J. *Langmuir* **2005**, *21*, 4896.
49. Sheng, P.; Wen, W. J. *Solid State Commun* **2010**, *150*, 1023.
50. Krzton-Maziopa, A.; Wycislik, H.; Plocharski, J. *J. Rheology* **2005**, *49*, 1177.
51. Cheng, Y. C.; Liu, X. H.; Guo, J. J.; Liu, F. H.; Li, Z. X.; Xu, G. J.; Cui, P. *Nanotechnology* **2009**, *20*, 055604.
52. Yin, J. B.; Xia, X.; Xiang, L. Q.; Zhao, X. P. *J. Mater. Chem.* **2010**, *20*, 7096.
53. Yin, J. B.; Zhao, X. P.; Xiang, L. Q.; Xia, X.; Zhang, Z. S. *Soft Matter* **2009**, *5*, 4687.
54. Wang, B. X.; Zhao, X. P. *Adv. Funct. Mater.* **2005**, *15*, 1815.
55. Wang, B. X.; Zhao, X. P. *Langmuir* **2005**, *21*, 6553.
56. Wang, B. X.; Zhou, M.; Rozynek, Z.; Fossum, J. O. *J. Mater. Chem.* **2009**, *19*, 1816.
57. Wang, B. X.; Rozynek, Z.; Fossum, J. O.; Knudsen, K. D.; Yu, Y. D. *Nanotechnology* **2012**, *23*, 075706.
58. Zhang, W. L.; Liu, Y. D.; Choi, H. J. *J. Mater. Chem.* **2011**, *21*, 6916.
59. Yin, Y. C.; Liu, C. J.; Wang, B. X.; Yu, S. S.; Chen, K. Z. *Dalton Trans.* **2013**, DOI:10.1039/C3DT32559H.